Microsyst Technol (2010) 16:411–421
DOI 10.1007/s00542-009-0966-3

TECHNICAL PAPER

Linewidth design rules for microstructures manufactured in PMMA resist using X-ray LIGA

Ron A. Lawes

Received: 24 June 2009 / Accepted: 24 November 2009 / Published online: 11 December 2009

Abstract During the past decade, individual simulation modules for the LIGA process have been developed, such as the power spectrum of the X-rays available from a given synchrotron, the effect of various components in the beam line, the image structure in the resist and image development. This has lead to an understanding of the parameters affecting the basic dimensional relationship between the mask and the 3D image in the resist itself. The commercialization of X-ray LIGA now requires knowledge of the parameters affecting the production engineering of micro devices. Foremost among these parameters are the manufacturing tolerances arising from variations in key microfabrication steps. This paper seeks to integrate the various physical simulation models into a single interactive program, whereby the design engineer can see the effect of different synchrotron output spectra, different beamline constructions and different resist parameters on the dimensions of the planned 3D microstructure. A novel approach to estimating the dimensional tolerances to be expected with large scale production is developed and comparison made with data available from the literature. Predicted results from using a particular synchrotron with a beamline designed to approximate to a "standard" exposure spectra at the rest surface are calculated, showing the microstructure shape and tolerance expected in large scale production. From these data a basic set of equations are established from which "Linewidth Design rules for LIGA" can be established. The steps following definition of the resist structure, for example electrodeposition, injection moulding or hot embossing, are not studied here.

R. A. Lawes (✉)
Optical and Semiconductor Devices Section,
Department of Electrical and Electronic Engineering,
Imperial College, Exhibition Road, London SW7 2BT, UK
e-mail: ronlawes@sachseln.plus.com

1 Introduction

Much of the science required for an understanding of X-ray LIGA technology has been extensively documented over the last 10–15 years including a variety of resist processes for both PMMA and SU-8 resists. Software has been developed to simulate the X-ray beam spectrum reaching the resist after modifying the synchrotron source by the effects of mirrors and aluminium absorbers in the beam line and the mask membrane and absorber pattern. A resist development simulator is available to ascertain the development conditions for a given exposure dose (Meyer et al. 2002a, 2003).

LIGA is now being evaluated for industrial applications and commercial exploitation, where a robust, cost effective manufacturing methodology is required. Efforts are being made to standardize the LIGA process in research laboratories such as FzK, Karlsruhe, CAMD, Louisiana and BESSY, Berlin (Mohr and Saile 2008; Loechel et al. 2007, 2008). Proposals have been made to produce masks with standardized dimensions to operate on a variety of synchrotron beam lines set up to minimize dimensional variations due to changes in the X-ray spectrum and beamline structure (Lawes 2008).

In order to take this work further, the X-ray LIGA model RALBEAM has been developed to take into account the advances made in LIGA simulation. RALBEAM now contains four key components:

(a) A synchrotron and beamline simulator capable of calculating the output of several of the world's

synchrotrons involved with LIGA and the beamline, along with its mirrors, absorbers and any air gaps.

(b) A module to simulate X-ray masks consisting of different membrane materials of different thicknesses, different resists (currently PMMA and SU-8) of any selected thickness and any gaps between mask and resist which are filled either with air or helium. The patterned X-ray absorber is usually gold, whose thickness can be varied to ensure non-exposure of the resist under the mask feature.

(c) A module to simulate the effect of variable development parameters (temperature and development time).

(d) A module to calculate the offset of the developed resist image with respect to the mask absorber edge at various depths throughout the resist thickness and hence the wall angle. The small effect of Fresnel diffraction may be included as an option.

Both a single absorber edge ($w \gg H$) and a specified linewidth ($w \ll H$) can be simulated.

RALBEAM is an Excel file, currently 24 MB in size, providing design interaction for the first three components of the model and calculations for component (*d*) leading to estimates for linewidth control and manufacturing tolerances. User interaction is via a "mimic" diagram which enables the various components to be chosen and the resultant X-ray spectrum to be examined. Table 1 lists the components that can be simulated and the related variables that can be set.

Drop-down menus are available for different synchrotrons (see next section), mirrors (different angles of incidence) and absorbers (different materials and thicknesses) in the beam line at different angles. Hence, the beam spectrum at the resist may be tailored to remove low and high energy X-rays and to achieve the required top-to bottom ratio of dose in the resist, particularly for PMMA. Absorption coefficients are available several authors (Henke et al. 1982; Hubbell and Seltzer 1996). In practice the difference between them is <2%.

For the scanner, mask and resist, the distance from the X-ray point source to the mask-resist assembly along with the horizontal and vertical beam angles will determine the horizontal and vertical dimensions of the scanning beam, respectively. A drop-down menu enables the mask membrane material (titanium, beryllium, carbon, silicon, silicon nitride or Kapton) to be chosen, along with its thickness. Air, vacuum, pressurized helium or Kapton may be chosen for the inter-resist gap. At present only PMMA and SU-8 resists are set up for analysis.

Table 1 Parameter variables that can be defined in RALBEAM simulator for synchrotron, beam line, scanner, mask, resist and supporting substrate

System	Component	Material	Parameter
Synchrotron	ANKA, ALS, BESSY 2, CAMD, Diamond, ElSA, NSCC, SRS, Subaru		Energy, current
Beam Line	Synchrotron Window	Be	Thickness
	Mirrors	Ni, Si, Cr	Angle
	Absorbers (2)	Al, Be, titanium, Kapton	Thickness
	Free space	Air, vacuum	Length
Scanner	Horizontal scan	Width	Angle and Window to resist distance
	Vertical scan	Height	
		Scan on/off times	seconds
		Number of Scans	
Mask	Absorber	Au	Thickness
	Membrane	Al, titanium, Be, C, Si, Si3N4, glass	Thickness
	Mask-resist separator	Air, helium, vaccum, Kapton	Thickness
Resist		PMMA, SU-8	Thickness
			Absorption coefficient
Exposure	Constant top dose		J/cm^3
	Constant bottom dose		J/cm^3
Developer	Post-exposure development	Standard PMMA and SU-8 Developer, e.g. GG	Development time and temperature
Substrate		Si, Al, Cu, Be	Thickness

2 Synchrotrons and beam lines

For each of these synchrotrons, the power spectra is provided as a pre-computed table defining the X-ray output as a function of energy, i.e. J/s/mRad$_{Horiz}$/eV. Figure 1 shows the output power and spectrum for a sample of synchrotrons from Table 2 at a fixed ring current of 100 mA. However, when running, each synchrotron may operate at a different ring current.

Diamond has been included to show the potential of third Generation synchrotrons to reduce exposure time for LIGA. Other synchrotrons are available in RALBEAM so that earlier publications can be investigated.

For many resist thicknesses LIGA exposure is ideally around 6,000 eV with minimal soft and hard radiations The beamline spectrum is moderated by including mirrors to eliminate high energy photons (e.g. >10,000 eV) from reaching the resist and an aluminium absorber to absorb sufficient soft X-rays to ensure that the Top-to-Bottom dose ratio is about 3 and the top dose $\ll$20,000 J/cm^3 for PMMA to avoid overheating. The absorber thickness will then only depend on the thickness of the resist. This ratio is less critical for SU-8 resist.

The result, shown in Fig. 2, is that the energy spread of the X-rays at the top surface of the resist is much more consistent from different synchrotrons, which will lead to similar shaped microstructures. The main difference between the synchrotrons is in the output power/eV at the resist, which will affect the time and hence the cost of exposure.

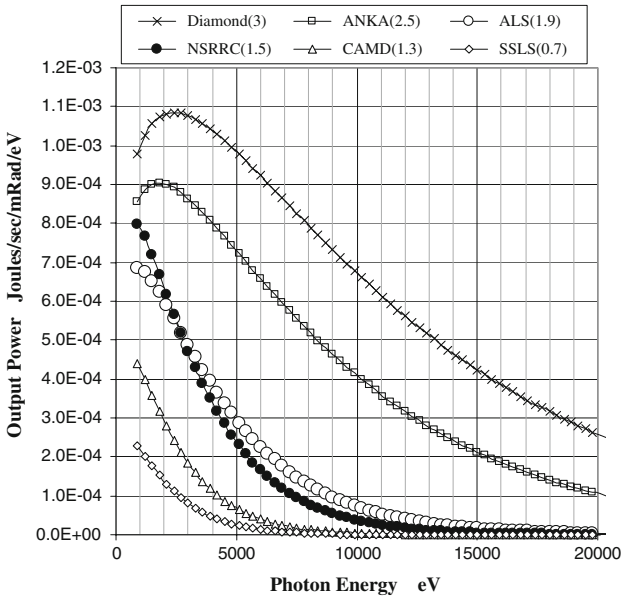

Fig. 1 Synchrotron output at 100 mA ring current

Table 2 Synchrotrons that have been used for LIGA and whose spectra are embodied in RALBEAM

Synchrotron	Country	Energy (GeV)	Field (Tesla)	SRing (mA)
ANKA	Germany	2.5	1.5	200
ALS	USA	1.9	1.27	400
BESSY 2	Germany	1.7	1.66	200
CAMD	USA	1.3	1.5	200
Diamond	UK	3.0	1.4	320
ELSA	Bonn	2.3	0.7	35
NSSRC	Taiwan	1.5	1.2	430
SRS	UK	2.0	2.0	200
SSLS	Singapore	0.7	4.5	300
Subaru	Japan	1.5	1.55	500

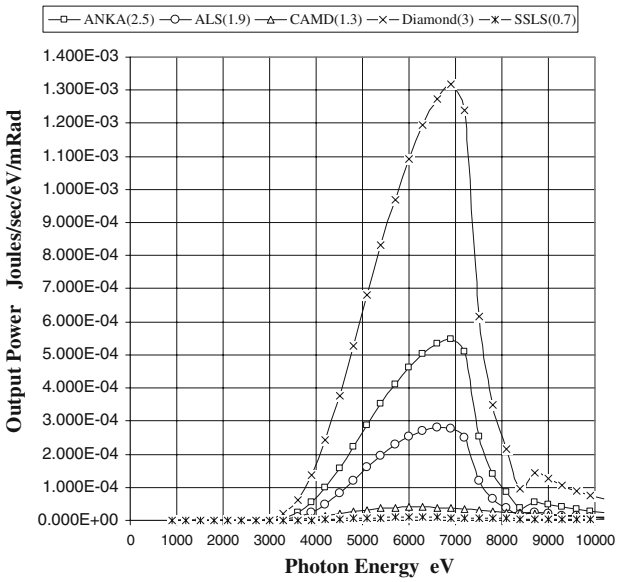

Fig. 2 X-ray energy at the resist top surface

3 Microstructure sidewall offsets and wall angles

The effect of the synchrotron energy spectrum and exposure dose has been simulated by RALBEAM to determine the resist image offset distances, relative to the edge of the mask feature, throughout the depth of the resist.

The lateral position of the image of the mask, at a given depth in the resist, is dependent upon the energy and magnitude of the X-rays. Thus at the top surface of the resist (O_T), the exposure dose is high, the full spectrum of the X-ray dose is available and secondary photoelectrons penetrate the maximum distance under the mask absorber edge. At the bottom of the resist (O_B), energy-dependent absorption of the softer X-rays reduces the magnitude of the exposure dose. The net effect causes less penetration under the mask edge (i.e. $O_T < O_B$). The offset varies as a function of depth into the resist between these two limits.

Table 3 Partial Coefficients and tolerances (standard deviation) at the top surface of the resist

Resist H	100	300	500	1,000
dL/dD_o (μm/Jcm^{-3}	0.012	0.017	0.018	0.021
Tolerance (nm)	5.8	7.9	9	9.8
dL/dH (μm/μm)	–	–	–	–
Tolerance (nm)	–	–	–	–
dL/dt (nm/min)	0.70	0.18	0.12	0.08
Tolerance (nm)	0.7	0.18	0.12	0.08
dL/dT (μm/°C)	8.0	11.25	12.5	15.0
Tolerance (Nm)	8.0	11.25	12.5	15.0
dX/α (μm/%)	–	–	–	–
Tolerance (nm)	–	–	–	–
dL/dMT (μm/°C)	5.97	5.64	5.67	5.72
Tolerance (Nm)	6	5.6	5.7	5.7
Total per Edge nm	11.5	15.1	16.1	18.8
Total line (nm)	23.1	30.1	32.2	37.7
Mask placement error (nm)	58	58	58	58
Total LIGA error (nm)	85	87	88	90

The irradiance at a depth (z) vertically into the resist, is given by:

$$J_{z(E)} = J_{0(E)} \exp(-\alpha_E z) \tag{1}$$

α = Absorption coefficient of PMMA as a function of energy (E) and

$J_{(0)} = \int_0^E J_{(0,E)} dE$ is the irradiance at the top of the resist (measured in mJ cm^{-2}) (Table 3).

The resist is exposed by the dose received, measured in J cm^{-3} at a depth z into the resist. The relationship between the dose and the irradiance is given by:

$$d(D(E,z)) = d(J)/\mathrm{d}z$$

$$D(z) = \int_0^E D_{0(E)} \alpha_{(E)} \exp(-\alpha_E, z)\mathrm{d}z \tag{2}$$

The basic theory of the magnitude of the sidewall offsets for PMMA, based upon the effect of electron penetration under the mask absorber edge, has been published (Griffiths 2004). The "half-kernel" theory therein described is embedded in RALBEAM, along with the option of including diffraction effects, as appropriate.

Based on the range and magnitude of electron penetration, the dose near the edge of the absorber is given by:

$$D(x,z) = \sum_{E1}^{E2} D_{(z)} \cdot \psi_{(\chi)} \tag{3}$$

Assuming the dose penetrating the mask absorber pattern is negligible:

$$\psi(E,z)) = 1/2 \cdot e^{-f} \quad (\chi \le 0) \tag{4}$$

$$\psi(E,z)) = 1 - 1/2 \cdot e^{-f} \quad (\chi \ge 0) \tag{5}$$

and

$$f = 3.34\chi + 5.5\chi^{3.84} \tag{6}$$

$$\chi = (x - x_o)/\gamma_E \tag{7}$$

γ_E is the electron range (in μ) in a resist for an initial energy E given by:

$$\gamma_{\mathrm{E}} = 1/\rho\left[(E/7.09)^{7.5} + (E/5.95)^{9.1}\right]^{0.2} \tag{8}$$

or $\gamma_{\mathrm{E}} = 2.215 \times 10^{-7}\ E^{-1.75}$ where $\rho = 1.19$ g/cm^3

Diffraction effects are often left out of LIGA calculations as the dimensional offsets due to photoelectrons tend to dominate. This is not necessarily true when considering deep sub-micron effects or in the case of high yield manufacture where a large gap between the mask and the resist might exist.

Diffraction for a line structure can be calculated from Eq. 3 and for an edge by setting $C_{(u1)} = S_{(u1)} = 0.5$

$$D(x,z) = 0.5\left\{[C(u2) + C(u1]^2 + [S(u2) + S(u1)]^2\right\} \tag{9}$$

where the Fresnel Number $u = x/\sqrt{0.5\lambda(g)}$,

u_1 and u_2 refer to the absorber position at $x = 0$ and $x = w$, respectively and $D_{(z)}$ is from Eq. 2.

$$C(u) = \int_0^u \cos(u^2\pi/2)\mathrm{d}u$$

$$S(u) = \int_0^u \sin(u^2\pi/2)\mathrm{d}u$$

X lateral distance in microns ($x = 0$ at the mask edge)
Z vertical depth into the resist in microns
g proximity gap between the mask and the top of the resist
λ wavelength of X-ray irradiation

The dose profile, due to photoelectrons and diffraction separately or together, can be calculated from RALBEAM (Fig. 3)

The sidewall can also be plotted as a function of depth (z) into the resist (Fig. 4 for a slit microstructure and Fig. 5 for a pillar.). Note the variation in offsets from top to bottom of the resist due to the significant absorption of dose with depth. The wall profile can be estimated by RALBEAM by plotting the offset as a function of the depth z into the resist and considering the effect of the developer conditions.

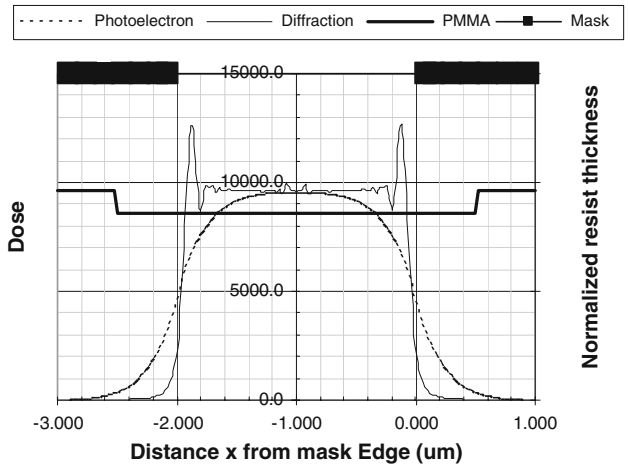

Fig. 3 Photoelectron and diffraction effects for a 2 μ slit in 500 μ of PMMA (ANKA LIGA 2 conditions)

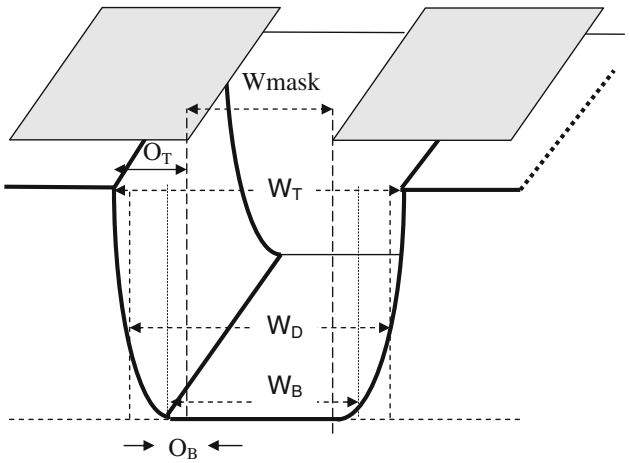

$$Wmask = W_D - (O_T + O_B)$$
$$W_{TOP} = W_D + (O_T - O_B)$$
$$W_{BOT} = W_D - (O_T - O_B)$$
$$Slope > (O_T - O_B)/H$$

Fig. 4 Parameters of a slit microstructure

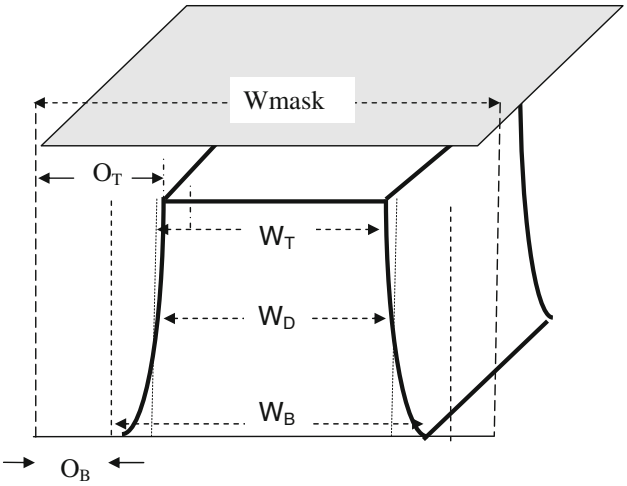

$$Wmask = W_D + (O_T + O_B)$$
$$W_{TOP} = W_D - (O_T - O_B)$$
$$W_{BOT} = W_D + (O_T - O_B)$$
$$Slope > (O_T - O_B)/H$$

Fig. 5 Parameters of a pillar microstructure

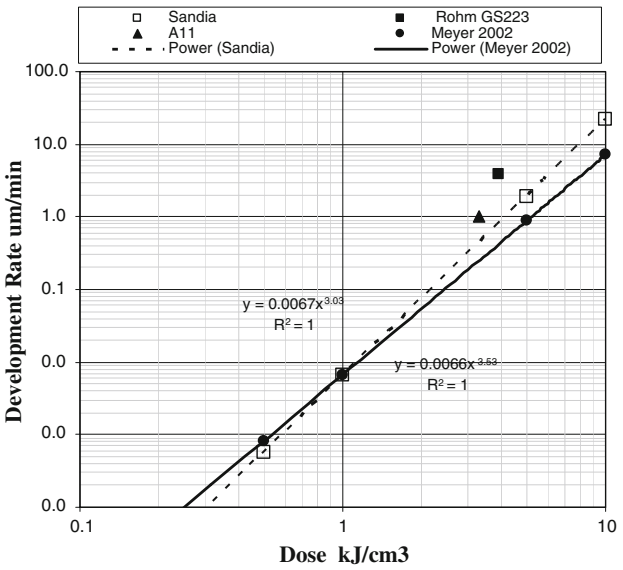

Fig. 6 Development rate versus exposure dose

4 Resist development

It has been shown by several authors (Mappes et al. 2006; Meyer et al. 2002b; Meyer et al. 1999) that the rate of development for PMMA is:

$$R_{(z)} = k_{(T)} D_{(z)}^{\beta(T)} \ \mu m/\min \quad (10)$$

The constants k and β depend upon the developer type (e.g. GG Developer), the developer temperature and the composition of the PMMA.

There is considerable variation in measurement of the constants k and β. Figure 6 shows the results from key publications that differentiate between versions of PMMA, including linear and cross-linked and developing methods (i.e. dip or megasonic development).

Two main studies of the development rate of PMMA enable the theory (Liu et al. 1998) and experiment (Pantenberg et al. 1998) of Eq. 10 to be assessed. Figure 6 shows reasonable agreement between data for a dose of 9.6 kJ/cm^3 and a development temperature of 21°C.

It is important to have adequate time after the development front has reached the bottom of the resist (e.g. T_{Dev} in the areas of maximum dose at the centre of the image) for the resist at the bottom of the feature's edge to develop.

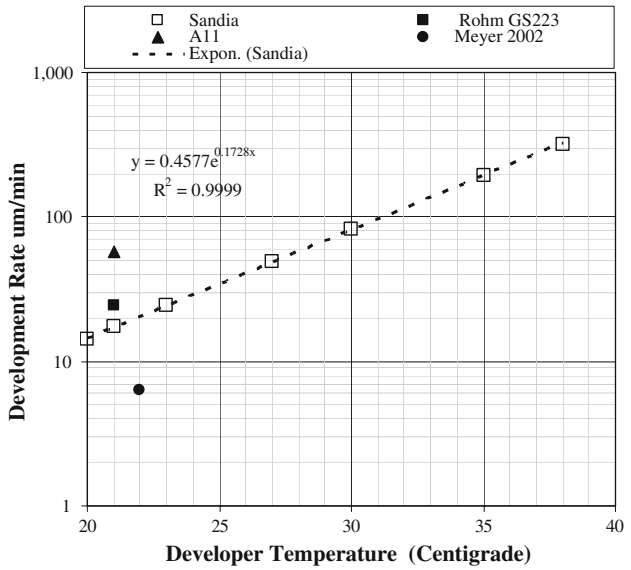

Fig. 7 Development rate versus temperature

In the subsequent calculations this is done by adding a fixed % of T_{Dev}.

$$T_{(\mathrm{Dev})} = (\exp(\alpha\beta H) - 1)/\left(\alpha\beta k_{(\mathrm{T})} D_{(z)}^{\beta(T)}\right) \tag{11}$$

$$\alpha = \ln(D_o/D_H)/H) \tag{12}$$

There is much variation of the parameters k and β in the literature and the effect of temperature. So PMMA development rate, as a function of temperature will be estimated from a range of experimental data, as shown in Fig. 7.

RALBEAM can use any of the development data available but for the rest of this study, linear PMMA will be assumed with:

$$\kappa = 2.96.10^{-3} e^{0.24T} \tag{13}$$

$$\beta = 4.26 - 0.03T \tag{14}$$

where T is the developer temperature in °C.

For example at 21°C

$$R_{(z)} = 4.96k \times 10^{-3} D_{(z)}^{3.6}\ \mu\mathrm{m/\,min} \tag{15}$$

This is the rate that PMMA will develop provided the dose is above the minimum threshold dose for bond scission (100–500 J/cm^2).

5 Computed edge offsets and wall angles

The magnitude of the edge offsets and wall angles will depend upon the spectrum and magnitude of the X-rays at the resist and can be computed by RALBEAM. A "model" beamline will be assumed to consist of the ANKA 2.5 GeV synchrotron as a source, a nickel mirror at an angle of

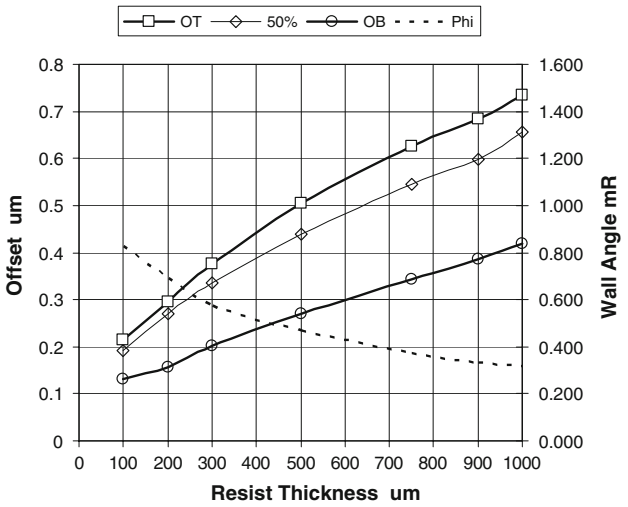

Fig. 8 Computed edge offsets and wall angles

7.85 mR to the beam and appropriate thickness aluminium absorbers to keep the top-to-bottom dose ratio in the PMMA resist at three. The surface dose is fixed at 9.6 kJ/cm^3. The X-ray beam will be delivered through a titanium mask membrane, 2.2 μm thick, with 25 μm gold absorber patterns. Development will be fixed at 21°C and the development time at 30% more than the calculated time for development to reach the bottom of the resist (T_{Dev}) in the areas of maximum dose.

The magnitude of the Offsets (refer to Figs. 4 and 5 for definitions) can be represented by (Fig. 8):

At the top of the resist

$$O_{\mathrm{T}} = 0.017H^{0.54} \tag{16}$$

At the bottom of the resist

$$O_{\mathrm{B}} = 0.011H^{0.52} \tag{17}$$

At the mid-thickness of the resist

$$O_{\mathrm{D}} = 0.017H^{0.53} \tag{18}$$

The wall angle (top to Bottom) is given by:

$$\varphi = 6.47H^{-0.53}\ \mathrm{mR} \tag{19}$$

Note. Computed values are positive for a slit, negative for a pillar microstructure and virtually identical in magnitude

6 Computed linewidth accuracy

As industrial applications become more production orientated, linewidth control and the minimum achievable dimensions become an essential part of the design rules for LIGA.

The linewidth simulation results are shown in Fig. 9 varying from 1 to 10 μm, in PMMA thicknesses varying

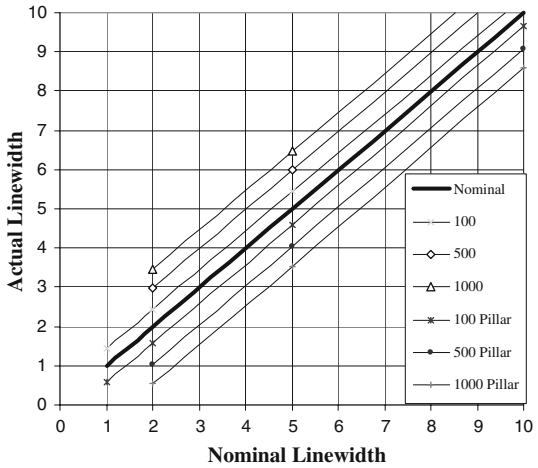

Fig. 9 Linewidth versus resist thickness (μ)

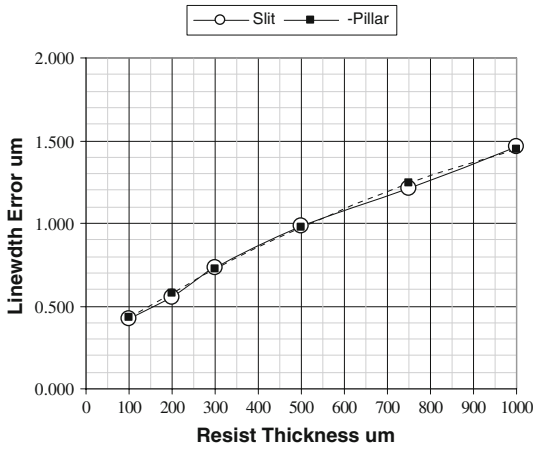

Fig. 10 Linewidth error for PMMA slits and pillars

from 100 to 1,000 μm. The linewidths at the top surface of the resist are shown for both slits and pillars.

The result becomes much clearer if the linewidth error ε, i.e. the resultant—nominal linewidth, is plotted as a function of resist thickness. Figure 10 shows the error varies with resist thickness according to:

$$\varepsilon = 0.034H^{0.54} \quad \text{(for a slit)} \tag{20}$$

$$\varepsilon = 0.035H^{0.54} \quad \text{(for a pillar)} \tag{21}$$

Note that the linewidth error is approximately equal but not identical to twice the top offset as electron–electron interactions make nanometre differences even at linewidths of 20–30 μm.

Equations 13 and 14 can be used by the mask maker to improve the linewidth accuracy, i.e. the CAD dimensions as designed should be decreased by a value calculated from Eq. 13 for designs consisting of only slit microstructures. Similarly, for designs consisting of only pillar microstructures, the CAD dimensions should be increased by a value calculated from Eq. 14. In practice these two equations give almost the same magnitude of correction, so that either value or an average may be used.

If employed, these mask corrections would enable the linewidth at the top of the resist to be accurate to ±10–90 nm, depending on the resist thickness.

For a design consisting of both slit and pillar features, the CAD must have some way of identifying which inflation/deflation factor should be used otherwise the linewidth error (Fig. 10) must be acceptable to the design.

7 Computed minimum linewidth dimensions

Linewidth control in semiconductor manufacture is often quoted to a specified fraction of the minimum linewidth in the design, for example ±5%. Both the dose and development conditions will affect the outcome. In the case of high aspect ratio microstructures, the thickness of the resist (H) and the wall angles, will together determine the linewidth achievable.

The minimum dimension that can be usefully used in LIGA design depends on the application. There may be different requirements for the top and bottom dimensions or of the wall angle. A typical design criterion is where the resist linewidth must be within a specified % (p) of the designed nominal X and Y dimensions of the microstructure.

Where the linewidth error ε must be accepted without mask correction, for example a mixture of slits and pillars in the same layer, then the minimum top surface dimension is given approximately by:

$$W_{\mathrm{MIN}} = 3.33p^{-1}H^{0.52} \quad \text{(for a slit)} \tag{22}$$

$$W_{\mathrm{MIN}} = 4.11p^{-1}H^{0.52} \quad \text{(For a pillar)} \tag{23}$$

Figure 11 illustrates the minimum linewidth at which ±5% dimensional control can be maintained. These estimates are much larger than those derived from less constrained criteria, where the processing conditions are carefully adjusted for special small scale applications.

Should the required microstructures be sufficiently simple, then the effect of the error may be compensated for in the CAD design of the mask. An even smaller linewidth may then be reproduced in PMMA, within a specified tolerance.

One option is to compensate fully for the resist top surface offset O_{T} thus modifying the dimension at the wall profile, and hence improving the tolerance. This is illustrated in Fig. 12. For example, in a 500 μm thick resist with complex patterns, the minimum slit dimension is approximately 18 μm for ±5% linewidth control. With simple shaped pattern this could be reduced to ±10 μm by mask dimension modification.

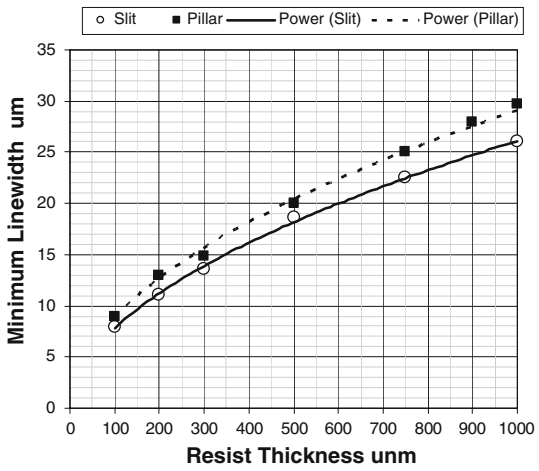

Fig. 11 Minimum dimensions as a function of resist thickness for a linewidth control of ±5%

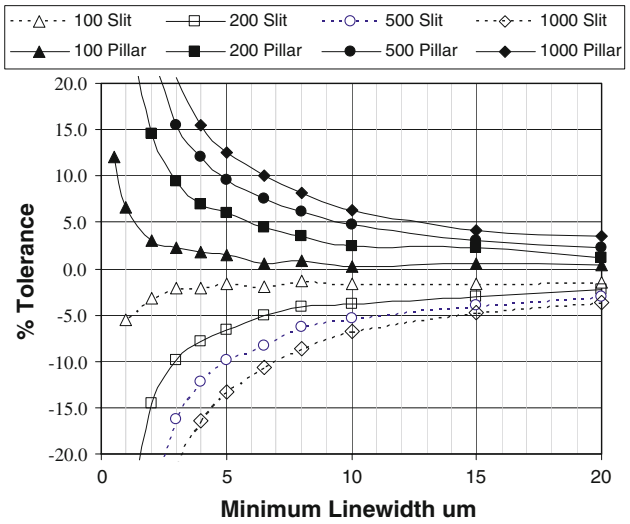

Fig. 12 Minimum linewidth, with the resist offset (O_{T}) compensated during mask generation

8 Computed manufacturing tolerances

The linewidths calculated above are those resulting from a fixed set of process conditions. These are systematic effects which do not take into account the random variations in the process conditions from batch to batch, month to month, etc.

Much of the scientific literature has concentrated on individual experiments to understand the physics underpinning LIGA. For LIGA to become more acceptable by industry, the sensitivity to the variation in key parameters must be studied. Little production information exists at present, so the methodology chosen here will be based upon a simple statistical approach to define the accumulation of tolerances.

The same approach will be adopted as for a previous analysis of UV LIGA (Lawes 2005) where partial coefficients of linewidth variations for a given fabrication parameter are estimated either from experimental data or the simulated relationships given in the analysis above. The results will be a good estimate of the tolerances expected in large scale manufacture providing all variations are relatively small and random.

The main variables that may affect linewidth control are

- the exposure irradiance and hence the resist dose. This will have an effect if there is an error in the mA min output of the synchrotron (σ_{D_0}).
- the resist thickness H (σ_H)

This will have no effect on the top surface of the resist but at the bottom of the resist ± errors in the resist height H will cause dimensional variations.

- the time of development, assuming a constant developer solution mixture ($\sigma_{t_{\mathrm{Dev}}}$).

This will have a minimal effect as the offset limit is at a low dose where the development rate is low (see Eq. 15)

- the developer temperature, which must be tightly controlled ($\sigma_{T_{\mathrm{Dev}}}$).
- the attenuation constant of the PMMA (σ_α).

There have been few studies in the literature to establish whether different batches of PMMA, prepared the same way, have different attenuation coefficients.

- the differential expansion between the mask and the resist as the mask-resist temperature varies (σ_{MT}).
- mask placement errors due to the grid structure of mask CAD and generation (σ_{MP}).

Provided each parameter is relatively small and statistically independent, then a simple statistical theory, combining all components in quadrature can be used:

$$\begin{aligned}\sigma_L^2 =& (dL/dD_0)^2\sigma_{D_0}^2 + (dL/dH\lambda)^2\sigma_H \\ &+ (dL/dT_{\mathrm{Dev}})^2\sigma_{T\,\mathrm{Dev}}^2 + (dL/dt_{\mathrm{Dev}})^2\sigma_{t_{\mathrm{Dev}}}^2 \\ &+ (dL/d\alpha)^2\sigma_\alpha^2 + (dL/dMT)^2\sigma_{\mathrm{MT}}^2 \\ &+ (\mathrm{dL/dMP})^2\sigma_{\mathrm{MT}}^2\end{aligned} \tag{24}$$

In the absence of any practical measurements, the partial coefficients will be obtained by simulation in RALBEAM.

Variations in the process parameters during manufacture (Table 2), are determined from reasonable estimates based on experience with routine production. These parameters

should be modified from specific measurements as data becomes available.

Preliminary estimates:

$$\sigma_{D_0} = \pm 5\%, \quad \sigma_H = \pm 10\,\mu\text{m}$$
$$\sigma_{t_{\text{Dev}}} = \pm 1\,\text{min} \quad \sigma_{T_{\text{Dev}}} = \pm 1^{\circ}\text{C}$$
$$\sigma_{\alpha} = \pm - 5\%$$
$$\sigma_{\text{MT}} = \pm - 1^{\circ}\text{C} \quad \sigma_{\text{MP}} = \pm 100\,\text{nm}$$

It will be seen that the dominant effects on linewidth variations are the temperature control of the developer, the temperature control of the mask-resist mechanical assembly and the placement accuracy of features on the mask. Variations in resist thickness and absorption coefficient have no effect on linewidth variations at the resist surface.

The contribution to the overall tolerance due to mask-resist temperature variation (*dL*/dMT) is a function of linewidth and, in Table 2, is calculated for a 100 μm slit estimate. The theory is derived from an analysis of a linear PMMA feature under stress (Griffiths et al. 2004), originally published as an explanation of resist swelling during development and adapted here to estimate the effect of heating during exposure. A similar analysis for a circular feature only produces a few nanometres difference at the dimensions under study here.

The mask placement error is caused by the grid structure used in the CAD design. Normally this is small enough to be ignored but it will be seen from Table 1 that the effect can be significant. For example a grid structure of 100 nm will produce an additional deviation of 58 nm ($100\sqrt{3}$).

Table 4 Partial coefficients and tolerances (standard deviation) at the bottom surface of the resist

Resist *H* (μm)	100	300	500	1,000
dL/dD_0 (μm/Jcm^{-3})	0.068	0.083	0.090	0.108
Tolerance (nm)	32.6	39.7	43.2	51.8
dL/dH (μm/μm)	−6	−4.2	−2.3	−1.4
Tolerance (nm)	−60	−42	−23	−14
dL/dt (nm/min)	2	1.2	0.33	0.43
Tolerance (nm)	2	1.2	0.33	0.43
dL/dT (μm/°C)	34.2	49.3	44	105
Tolerance (Nm)	34.2	49.3	44	105
dX/α (μm/%)	−0.6	−1.2	−2	−2.8
Tolerance	−3	−6	−10	−14
dL/dMT (μm/°C)	–	–	–	–
Tolerance (Nm)	–	–	–	–
Total per edge (nm)	71.3	69.4	92.9	108.3
Total line (nm)	143	139	186	217
Mask placement error (nm)	58	58	58	58
Total LIGA error (nm)	164	161	203	232

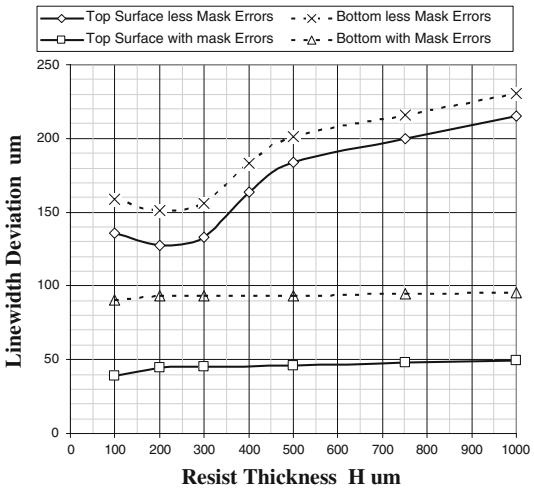

Fig. 13 Linewidth variations as a function of resist thickness (note nanometer scale)

A similar analysis can be done for the bottom of the resist as summarized in Table 4. Variations in exposure dose, resist thickness, developer temperature and mask placement error make significant contributions to a much larger overall effect. Changes in the attenuation coefficient of PMMA result in a small effect. Mask-resist temperature variations are assumed to have no effect as the resist is constrained by adhesion to the substrate.

Figure 13 shows the approximate linewidth variations, for the given fabrication parameters.

Efforts to reduce each of these manufacturing parameters could result in a dimensional tolerance below 100 nm at 3σ.

9 Manufacturing tolerances in large scale production

A definitive experiment requires a large sample of "identical" microstructures, where all relevant parameters are specified, along with their variations during production runs, day to day, week to week, etc. This has yet to be done and/or published.

The best data published to date comes from the extensive work at FzK, Karlsruhe fabricating gear wheels for the watch industry (Meyer et al. 2008). Plotting Fig. 5 of that publication as a distribution, a bi-modal distribution is obtained, as shown in Fig. 15 here. The reference estimates the mask dimensions to be 302.9 ± 0.18 μm and the standard deviation of the measuring error to be ±0.1 μm.

Discussions with the authors reveal that exposures were done both at ANKA and at BESSY where cooling of the substrate was temporarily faulty during fabrication by many tens of degrees. This would explain the presence and magnitude of a second distribution. Hence, the result may

be considered as the sum of two Gaussian distributions, a core distribution representing the expected result from volume production and a similar distribution shifted by the result of occasional poor cooling of the mask-resist assembly.

The difference between the average of the two distributions is 304.3–303.6 = 0.7 μm, which could be caused by a temperature rise of 0.700/16.9 = 41°C.

From the raw data for the core distribution:

$$\text{Average}_{\text{Core}} = 303.6\,\mu\text{m}$$
$$\sigma_{\text{Core}} = 0.25\,\mu\text{m}.$$

The gear wheels manufactured have a final height of 900 μm. Assuming the average mask dimension will be increased by the amount derived from Eq. 16 (0.7 μm) and the standard deviation by the amount calculated from Table 2 for a 300 μm diameter linewidth, then from theory, the measured dimensions should be:

$$\text{Average}_{\text{Core}} = 302.9 + 0.7 = 303.6\,\mu\text{m}$$
$$\sigma_{\text{Core}} = \sqrt{\left(0.037^2 + 0.18^2 + 0.1^2\right)} = 0.21\ \mu\text{m}$$

This is in good agreement with the core measurements in Fig. 14.

Predictions can be made for the potential of LIGA to produce extremely low tolerances in production.

Ignoring the mask and measuring errors, the gear wheels appear to have an intrinsic deviation:

$$\sigma_{\text{Core}} = 0.14\,\mu\text{m} \quad \text{i.e.}\sqrt{\left(0.25^2 - 0.18^{2-}0.1^2\right)}.$$

The average top surface dimension in PMMA can be achieved within the placement accuracy of the mask, e.g. 58 nm, by mask dimension compensation. The standard deviation at the top surface would be 50–100 nm, depending on the mask grid structure. Under these conditions the bottom of the resist will have an average dimension of 303.3 μm (302.9 + 0.4) and a standard deviation of 0.22 μm (see Eq. 18 and Table 4).

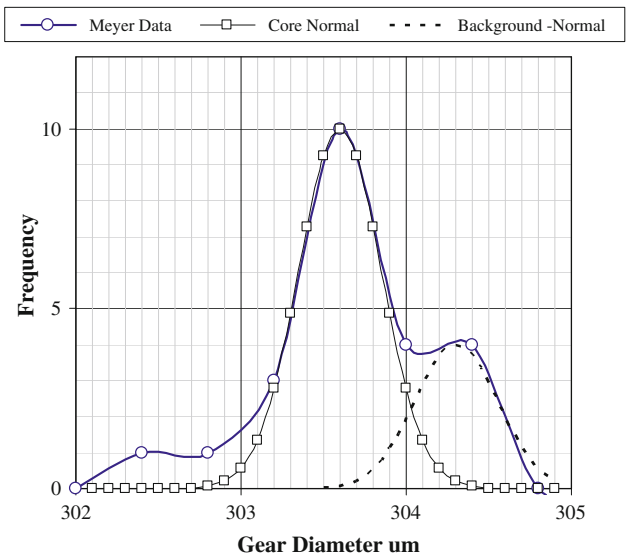

Fig. 14 Process reproducibility of the diameter of a gear wheel in a sample of 20 wafers (Meyer et al. 2008)

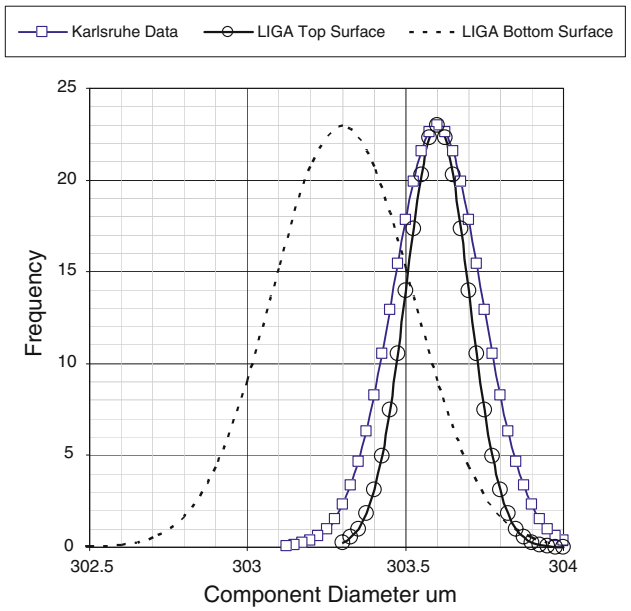

Fig. 15 Process reproducibility of the diameter of a gear wheel in a sample of 20 wafers from theory

These results are plotted in Fig. 15.

The deviation at the bottom of the resist is much greater than at the top and can be reduced by increasing the development time. This would also increase the top surface offset, resulting in an increase in the minimum dimension. In many applications this might be acceptable.

10 Discussion

A methodology has been developed to predict the tolerances in 3D microstructures in large scale production and so provide a basis for sets of design rules.

The methodology is based on simulation of a synchrotron, a standard beamline delivering a known X-ray spectrum to the PMMA resist, a theoretical model for electron penetration under the mask edge and for a resist development model based on PMMA. The relatively small effect of diffraction can be included in the simulation software RALBEAM, where sub-micron linewidths with large mask to resist gaps are involved.

The offset error between the defining mask edge and the resultant rest edge after development can be determined at any depth (z) into the resist, along with the wall angle. This error could be reduced or eliminated for simple shapes by modifying the mask dimension at manufacture but only for

a given position, e.g. the top surface. Thus, simple design rules can be used to control the linewidth at the x, y and z dimensions, depending on the application. For example, Eqs. 19 and 20 enable the design rules for the wall profile of the microstructures to be predicted and Eqs. 21 and 22 the error in average linewidth.

Sub-micron linewidth definition is often claimed for X-ray LIGA but this is not practical for many applications, where linewidth tolerance is a key parameter. The minimum linewidth is a function of resist thickness and the tolerance required. For example, a tolerance of ±5% in a resist thickness of 500 μm is only possible with linewidths greater than 19 μm.

Section 8 estimates the tolerances that should be included in the design rules to ensure a minimum yield from manufacture. The new features of the RALBEAM simulator enable estimates to be made using partial coefficients and measurements or estimates of variation.

RALBEAM has been used to simulate LIGA manufacture at the ANKA synchrotron, from which production measurements are available. Using a typical beamline to deliver a dose of 9,600 J cm^{-3} at the top of a PMMA layer of varying thickness, results have been calculated for actual linewidths with respect to the CAD design, and the minimum useful linewidth.

There is good agreement with the published data but further experimentation is required, not only to gather data to confirm the theory of tolerances in large scale production, but also to confirm the value of the partial coefficients outlined.

Several effects have not been included in this study. Resist swelling (Griffiths et al. 2004) has not been taken into account and may become important as dimensions and required tolerances become smaller. In particular, tolerances after electro deposition have not been included in the model, where resist swelling and other effects may alter final dimensions.

Parameters, such as exposure dose, developer temperature and time, mask design and mask-wafer temperature control, contribute significantly to linewidth control.

Acknowledgments The detailed analysis of sidewalls and hence linewidth would not have been sufficiently accurate without the general theory undertaken by SK Griffiths at Sandia Laboratory. The difficult task of demonstrating reasonable agreement between the integrated theory developed in this paper with experimental results would have been impossible without the quality measurements coming from the work of Volker Saile and his team at FzK, Karlsruhe including giving the author early sight of some their latest, unpublished results.

References

Griffiths SK (2004) Fundamental Limitations of LIGAXray lithography: sidewall offset, slope and minimum feature size. J Micromech Microeng 14(7):999–1011

Griffiths SK, Crowell JW, Kistler BL, Dryden AS (2004) Dimensional errors in LIGA-produced metal structures due to thermal expansion and swelling of PMMA. J Micromechan Microeng 14(7):999–1011

Henke BL, Lee P, Tanoka T, Shimabukara R, Fujikawa B (1982) Atomic data and nuclear data tables, vol 27, pp 1–144

Hubbell JH, Seltzer SM (1996) Tables of X-ray mass attenuation coefficients. National Institute of Standards and Technology NISTIR 5632

Lawes RA (2005) Manufacturing tolerances for UV LIGA using SU-8 resist. J Micromech Microeng 15:2198–2203

Lawes RA (2008) A traceable fabrication process for X-ray LIGA. Int J Nanomanuf 2(6):572–582

Liu Z, Bouamrane F, Roilly M, Kupta RK, Labeque A, Megtert S (1998) Resist dissolution rate and inclined wall structures in deep X-ray lithography. J Micromech Microeng 8:293–300

Loechel B, Gottert J, Desta YM (2007) Direct LIGA service for prototyping—status report. Microsyst Technol 13:327–334

Loechel B, Gottert J, Gruetzner G, Bednarzik M, Waberski C, Ahrens G, Engelke R, Singh V, Degen R, Kirsch (2008) Extreme aspect ratio NiFe gear wheels for the production of commercially available Micro harmonic Drive gears. Microsyst Technol 14:1675–1681

Mappes S, Achenbach JM (2006) Process conditions in X-ray lithography for the fabrication of devices with submicron feature sizes. Microsyst Technol 13:355–360

Meyer P, El-Kholi A, Mohr J, Cremers C, Bouamrane F, Megtert S (1999) Study of the development behaviour of irradiated foils and microstructure. SPIE 3874:312–320

Meyer P, Cremers C, El-Kholi A, Haller D, Schulz J, Hahn L, Megtert S (2002a) A MS-Windows simulation tool for synchrotron X-ray exposure and subsequent development. Microsyst Technol 9:104–108

Meyer P, El-Kholi A, Schulz J (2002b) Investigations of the development rate of irradiated PMMA microstructures in deep X-ray lithography. Microelectron Eng 63:319–328

Meyer P, Schulz J, Hahn L (2003) DoseSim: Microsoft Windows graphical user interface for using synchrotron X-ray exposure and subsequent development in the LIGA process. Rev Sci Instrum 74(2):1113–1118

Meyer P, Schulz J, Hahn L, Saile V (2008) Why will you use the deep X-ray LIGA technology to produce MEMS? Microsyst Technol 14:1548–1557

Mohr J, Saile V (2008) ANKA annual report, pp 135–136. http://www.anka-cos.kit/edu

Pantenberg FJ, Achenbach S, Mohr J (1998) Influence of developer temperature and resist material on the structure quality in deep X-ray lithography. J Vac Sci Technol B 16(6):3547–3551